Clinical Investigations

Quantitation of the Mitral Tetrahedron in Patients With Ischemic Heart Disease Using Real-Time Three-Dimensional Echocardiography to Evaluate the Geometric Determinants of Ischemic Mitral Regurgitation

Address for correspondence:
Lung-Chun Lin, MD
Echocardiography Laboratory,
Cardiovascular Center
National Taiwan University Hospital
No. 7 Chung-Shan South Road
Taipei 100, Taiwan
anniejou@ms28.hinet.net

Chin-Feng Hsuan, MD; Hsi-Yu Yu, MD, PhD; Wei-Kung Tseng, MD, PhD; Lung-Chun Lin, MD, PhD; Kwan-Lih Hsu, MD, PhD; Chau-Chung Wu, MD, PhD
Division of Cardiology, Department of Internal Medicine (Hsuan, Tseng, Hsu), E-Da Hospital, I-Shou University, Kaohsiung, Taiwan; Department of Surgery (Yu), National Taiwan University Hospital, Taipei, Taiwan; Division of Cardiology, Department of Internal Medicine (Lin, Wu), National Taiwan University Hospital, Taipei, Taiwan

ABSTRACT

Background: Ischemic mitral regurgitation (IMR) is common in ischemic heart disease and results in poor prognosis. However, the exact mechanism of IMR has not been fully elucidated.

Hypothesis: Quantitation of the mitral tetrahedron using three-dimentianl (3D) echocardiography is capable of evaluating the geometric determinants and mechanisms of IMR.

Methods: Forty patients with a history of ST-elevation myocardial infarction at least 6 months earlier were studied. Parameters of mitral deformation and global left ventricular (LV) function and shape were evaluated by 2-dimensional echocardiography. The effective regurgitant orifice (ERO) of IMR was obtained by the quantitative continuous-wave Doppler technique. Three-dimensional (3D) echocardiography was applied to assess the mitral tetrahedron.

Results: Mitral valvular tenting area ($P < 0.001$), mitral annular area ($P = 0.032$), dilation of the LV in diastole, impairment of the LV ejection fraction, and volume of the spherically shaped LV in systole were greater in patients with an ERO $\geq$20 mm^2 than in those with an ERO $<$20 mm^2. In the mitral tetrahedron, only the interpapillary muscle roots distance showed a significant difference ($P = 0.004$). Multivariate analysis with the logistic regression model showed the systolic mitral tenting area (odds ratio [OR]: 280.49, 95% confidence interval [CI]: 4.59-1.72 $\times$ 10^4, $P = 0.007$) and interpapillary muscle distance (OR: 1.50, 95% CI: 1.03-2.19, $P = 0.036$) to be independent factors in predicting significant IMR (ERO $\geq$20 mm^2).

Conclusions: 3D echocardiography can be effectively applied in measuring the mitral tetrahedron and evaluating the mechanism of IMR. Mitral valvular tenting and interpapillary muscle distance are 2 independent factors of significant IMR.

Introduction

Ischemic mitral regurgitation (IMR) is frequently presented in ischemic heart disease with left ventricular dysfunction despite a structurally normal mitral valve.[1] The presence of IMR after myocardial infarction (MI), in acute or chronic phase, is associated with a significant increase in the risk of death and heart failure.[2–4] However, the mechanism and treatment of IMR has not been fully elucidated. Papillary muscle dysfunction causing mitral valve prolapse has previously been proposed as the cause of IMR.[5] However, in animal and clinical studies, isolated papillary muscle dysfunction failed to generate IMR.[6–9] Recently, Godley and He et al. demonstrated that incomplete mitral leaflet closure may be the primary mechanism.[10,11] Left ventricular (LV) dilatation, LV systolic dysfunction, mitral annular dilatation or dysfunction, and local LV remodeling with papillary muscle displacement have been postulated to involve the incomplete mitral leaflet closure and the generation of IMR.[6,11–15] However, these recent studies used 2-dimensional (2D) echocardiography to assess the local or global remodeling and the annular geometry. There are

The authors have no funding, financial relationships, or conflicts of interest to disclose.
Additional Supporting Information may be found in the online version of this article.

Clin. Cardiol. 36, 5, 286–292 (2013)
Published online in Wiley Online Library (wileyonlinelibrary.com)
DOI:10.1002/clc.22111
Received: November 16, 2012
Accepted: February 9, 2013

several limitations with 2D imaging that include an inability to provide accurate surgical views and partial quantitation.[16] Yu et al. used magnetic resonance imaging (MRI) as a method to assess the geometry of the mitral apparatus and proposed mitral tetrahedron as a geometrical surrogate for IMR.[17] A mitral tetrahedron is defined by its 4 vertices at the medial, lateral papillary muscle roots, and the anterior and posterior mitral annulus, and therefore it is encompassed by 6 edges (Figure 1). A study by Yu et al. that involved patients with ischemic cardiomyopathy and advanced ventricular remodeling, demonstrated that the whole mitral tetrahedron (elongated 6 edges) is a significant geometric surrogate for chronic IMR.[18] However, MRI also has some disadvantages in evaluating IMR, including: (1) poor resolution for valvular structures, (2) inability to evaluate IMR severity, (3) cost, and (4) time. Yet, advancements in 3-dimensional (3D) echocardiography provide another method to assess the spatial relationship of the mitral apparatus. The primary purpose of this study was to determine the capability of real-time 3D echocardiography in measuring the 6 edges of mitral tetrahedron in patients with IMR after MI. The secondary goals were to evaluate the possible determinants for IMR by traditional 2D echocardiography and by newer 3D echocardiography methods and to compare the weight of each determinant on the severity of mitral regurgitation (MR) after MI.

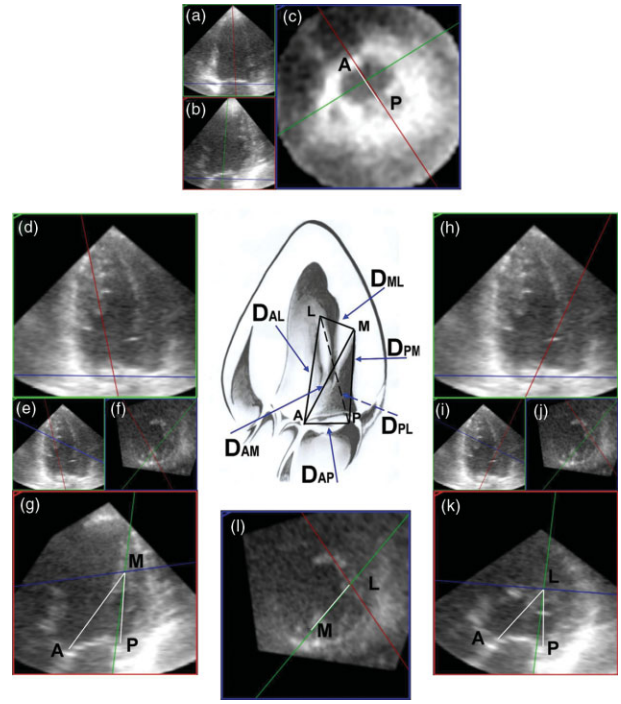

Figure 1. Measurement of the mitral tetrahedron. First, the maximal left ventricular (LV) contraction was defined as the end-systolic phase. An anteroposterior plane (red frame) that passed through the anterior and posterior annulus was adjusted to parallel the LV axis (part a). Another plane (green frame) perpendicular to the anteroposterior plane was also adjusted to parallel the LV axis (part b). Then, a horizontal plane (blue frame) was accommodated to the mitral ring by the assistance of these 2 planes (part c). The distance between the anterior and posterior annulus (D_{AP}) was measured, and the long-axis of mitral annulus was also obtained. The mitral annular plane (part c) was annotated to form the reference plane for tilting the anteroposterior plane. Second, the blue frame was moved to the level of the roots of the papillary muscles and intersected with the green frame. These 2 frames were moved carefully to define the exact point of the roots of papillary muscles (part l). The blue frame at this time was annotated to be the papillary muscle roots plane. The anteroposterior plane (red frame) was tilted to the root of medial papillary muscle using a reference hinge intersecting by the mitral annular plane and the anteroposterior plane (part d). The exact intersection of anteroposterior plane with the root of the medial papillary muscle was assisted by the green frame and the papillary muscle roots plane (parts e and f). On the anteroposterior plane imaging (part g), the intersecting point of the blue and green line was the root of medial papillary muscle (M) (part g), and the distance between the root of medial papillary muscle and the anterior annulus (D_{AM}) and the posterior annulus (D_{PM}) could be measured. By the same way, the distance between the root of lateral papillary muscle and the anterior annulus (D_{AL}) and the posterior annulus (D_{PL}) could be measured after tilting the anteroposterior plane to the root of lateral papillary muscle (parts h–k). Finally, the interpapillary muscle roots distance (D_{ML}) could be measured on the papillary muscle roots plane (part l). Abbreviations: M, the root of medial papillary muscle; L, the root of lateral papillary muscle; A, the anterior annulus; P, the posterior annulus.

Methods

Study Population

The study population was comprised of 40 consecutive patients from 2005 to 2006, each of whom had a history of ST-elevation MI >6 months. The diagnosis of MI was made on the basis of history, electrocardiography, and elevation of cardiac enzymes. The location of the MI was according to the leads of the ST-segment elevation. The time interval between infarction and echocardiographic assessment was > 6 months for all patients. Exclusion criteria were: structural mitral lesions, clinical or echocardiographic evidence of other cardiac disease, more than trace aortic regurgitation, suboptimal echocardiographic windows, and atrial fibrillation or other arrhythmia interfering in the acquisition of images. Patients recruited into the study gave informed consent, and the study was approved by the institutional review board of the National Taiwan University Hospital.

2D Echocardiographic Measurements

Echocardiographic studies were performed using a Phillips Sonos 7500 (Philips Medical Systems, Bothell, WA) ultrasound system. All 2D echocardiographic images and Doppler data were obtained with a S3 probe and digitally stored on optical discs for offline analysis. Left ventricular end-diastolic volume (LVEDV), LV end-systolic volume, and LV ejection fraction (LVEF) were measured by the biplane Simpson disc method.[19] The sphericity index was defined as the ratio of short- to long-axis dimension of the LV from the apical 4-chamber view at end-systole.[20] The mitral valvular tenting area was measured as an area enclosed between the annular plane and the mitral leaflets.[15] The mitral valvular tenting area was obtained from the parasternal long-axis view at end-systole.

The quantitative continuous-wave Doppler technique was used to quantify MR. The mitral and aortic stroke volumes were calculated to derive the mitral regurgitant volume

Published online in Wiley Online Library (wileyonlinelibrary.com)
DOI:10.1002/clc.22111

(RV).[21,22] The effective regurgitant orifice (ERO) was obtained by dividing the RV by the regurgitant time-velocity integral.[23] An ERO $\geq 20\ mm^2$ in patients with IMR adversely predicts long-term clinical outcome.[3,4] Therefore, an ERO $\geq 20\ mm^2$ was used to determine the significance of MR; subsequently, the patients were classified into 2 groups: ERO $<20\ mm^2$ and ERO $\geq 20\ mm^2$.

3D Echocardiographic Measurements

The Phillips Sonos 7500 (Philips Medical Systems) ultrasound system was used to obtain transthoracic volumetric images with an ×4 probe in the apical view in all studied patients. The transducer position was adjusted carefully to ensure its location at the apex and to include the entire LV and mitral valve in both imaging planes using a biplane mode. Next, the full-volume image was acquired and digitally stored on compact disks for offline analysis. The volumetric frame rate was 16 to 22 frames per second, with an imaging depth of 12 to 16 cm. We used 3D computer software (3DQ, QLAB version 4.1; Philips Medical Systems) to define the mitral tetrahedron (Figure 1). The distance between the anterior and posterior annulus (D_{AP}), the long-axis of mitral annulus ($D_{long\text{-}axis}$), the distance between the root of medial papillary muscle and the anterior annulus and the posterior annulus, the distance between the root of lateral papillary muscle and the anterior annulus and the posterior annulus, and the interpapillary muscle roots distance (D_{ML}) were measured. Mitral annular area was calculated as $\pi(D_{AP} \times D_{long\text{-}axis})/4$. The offline measurement of mitral tetrahedron was performed by a single experienced sonographer (Chin-Feng Hsuan).

Evaluation of Reproducibility

Reproducibility for the measurement of the 6 edges of the mitral tetrahedron was assessed in 20 patients. Intraobserver variability was performed by the author. Another experienced sonographer (Lung-Chun Lin) measured the mitral tetrahedron for the interobserver variability.

Statistics

Continuous variables are expressed as mean ± standard deviation percentages for categorical data. Group comparisons were performed with the Student t test, Pearson χ^2 test, or Fisher exact test as appropriate. Interobserver and intraobserver variability in measuring edge length were presented as inter- and intracorrelation coefficients (ICC_{inter} and ICC_{Intra}) and expressed as the standard error of estimation of ICCs. The correlation of ERO measurement with echocardiographic variables was performed using the Pearson correlation analysis. Furthermore, a stepwise logistic regression analysis was performed to identify the risk factors associated with ERO. Univariate logistic regression was analyzed to determine the association of ERO levels with echocardiographic variables. Variables with a P value <0.2 from univariate logistic regression analysis were put into multivariate logistic regression analysis with a backward stepwise conditional selection. All statistical assessments were 2-tailed and considered statistically significant if $P < 0.05$. All statistical analyses were performed with SPSS 18.0 for Windows (IBM, Armonk, NY).

Table 1. Demographic Data of the Study Group

Variables	ERO $<20\ mm^2$ (n = 24)	ERO $\geq 20\ mm^2$ (n = 16)	P Value
Age, y	56.79 ± 7.58	57.31 ± 9.21	0.846
Gender			0.638
Male	21 (87.5)	15 (93.8)	
Female	3 (12.5)	1 (6.3)	
BMI, kg/m^2	24.66 ± 2.35	24.76 ± 2.07	0.893
BSA, cm^2	1.76 ± 0.16	1.79 ± 0.16	0.555
CPK, IU/mL	4589.88 ± 2266.59	6180.75 ± 3627.92	0.095
Location of myocardial infarction, %			0.027[a]
Inferior	9 (37.5)	12 (75)	
Anterior	15 (62.5)	4 (25)	
Smokers, %	15 (62.5)	11 (68.8)	0.685
Hypertension, %			0.151
Yes	8 (33.3)	9 (56.2)	
No	16 (66.7)	7 (43.8)	
Diabetes mellitus, %			0.717
Yes	6 (25)	3 (18.8)	
No	18 (75)	13 (81.2)	
Dyslipidemia, %			0.121
Yes	15 (62.5)	6 (37.5)	
No	9 (37.5)	10 (62.5)	

Abbreviations: BMI, body mass index; BSA, body surface area; CPK, creatinine phosphokinase; ERO, effective regurgitant orifice.
Continuous data are presented as mean ± standard deviation and categorical data as n (%).
[a] $P < 0.05$, indicated significantly different between ERO levels.

Results

Demographics of Study Population

The study population consisted of 40 patients (36 males and 4 females). Age, body mass index, and body surface area were comparable between groups (Table 1). Table 1 presents the patients characteristics by ERO levels: ERO $<20\ mm^2$ and ERO $\geq 20\ mm^2$. Patients with an ERO $\geq 20\ mm^2$ had a higher rate of inferior location compared to those with an ERO $<20\ mm^2$ ($P = 0.027$).

Reproducibility of Measurements

The intraobserver and interobserver variability was comparable when measuring the edge length of the mitral tetrahedron in 20 patients (Table 2). This implies that there was good reproducibility of measurement regardless of the operator.

Published online in Wiley Online Library (wileyonlinelibrary.com)
DOI:10.1002/clc.22111

Table 2. Inter- and Intraobservational Variability in Measuring Edge Lengths

Edge Length of Mitral Tetrahedron, mm	Interobservational Variability[a]		Intraobservational Variability[a]	
	ICC_{inter}[b]	SEE	ICC_{Intra}[b]	SEE
D_{AP}	0.72	1.16	0.77	1.08
D_{AL}	0.92	2.63	0.91	2.77
D_{AM}	0.89	2.61	0.93	2.11
D_{PL}	0.89	2.59	0.97	1.49
D_{PM}	0.93	1.86	0.95	1.67
D_{ML}	0.90	1.89	0.97	1.1

Abbreviations: D_{AL}, the distance between the root of lateral papillary muscle and the anterior annulus; D_{AM}, the distance between the root of medial papillary muscle and the anterior annulus; D_{AP}, distance between the anterior and posterior annulus; D_{ML}, the interpapillary muscle roots distance; D_{PL}, the distance between the root of lateral papillary muscle and the posterior annulus; D_{PM}, the distance between the root of medial papillary muscle and the posterior annulus; SEE, standard error of estimation.
[a]Inter- and intraobservational variability presented as inter- and intracorrelation coefficients (ICC_{inter} and ICC_{Intra}) with SEE of ICCs. [b]All ICCs are significant with a P value <0.001.

Measurements of Mitral Deformation, LV Remodeling, and the Mitral Tetrahedron

Table 3 shows the association of ERO levels with echocardiographic variables. The data show that the patients in the ERO $\geq$20 mm^2 group had a greater tenting area, mitral annular area, LVEDV, and spherical index at systole compared with the ERO <20 mm^2 group ($P < 0.05$). Conversely, LVEF was greater in the ERO <20 mm^2 group compared with the ERO $\geq$20 mm^2 group ($P < 0.05$). Furthermore, with regard to the edge length of the mitral tetrahedron, the D_{ML} was also significantly greater in patients with a high ERO level compared to those with a low ERO level. (25.38 ± 5.92 vs 20.29 ± 2.65 mm, $P = 0.004$).

Determinants of the Severity of IMR

Overall, the ERO measurement was positively correlated with tenting area ($r = 0.574$, $P < 0.001$), LVEDV ($r = 0.352$, $P < 0.05$), spherical index at systole ($r = 0.458$, $P < 0.01$), and D_{ML} of edge length of mitral tetrahedron ($r = 0.449$, $P < 0.01$) (Table 4). There was a negative ERO measurement correlation with LVEF (-0.279, $P = 0.081$), although it was not statistically significant.

The univariate and multivariate logistic regression analysis for identifying the risk factors associated with significant IMR (ERO $\geq$20 mm^2 vs <20 mm^2) are summarized in Table 5. The stepwise logistic regression analysis shows that significant IMR was significantly associated with tenting area (odds ratio [OR]: 280.49, 95% confidence interval [CI]: 4.59-1.72 $\times 10^4$, $P = 0.007$] and D_{ML} (OR: 1.50, 95% CI: 1.03-2.19, $P = 0.036$).

Table 3. Patients' Echocardiographic Variables by ERO Level

Variables	ERO <20 mm^2 (n = 24)	ERO $\geq$20 mm^2 (n = 16)	P Value
Tenting area, cm^2	0.61 ± 0.24	0.99 ± 0.29	<0.001[a]
Mitral annular area, cm^2	6.44 ± 0.98	7.13 ± 0.95	0.032[a]
LVEDV, mL	70.49 ± 18.52	88.06 ± 33.36	0.039[a]
LVESV, mL	28.51 ± 12.28	45.74 ± 33.62	0.065
Spherical index at systole	0.40 ± 0.09	0.49 ± 0.09	0.004[a]
LVEF, %	61.23 ± 7.53	52.64 ± 14.46	0.041[a]
Edge length of mitral tetrahedron, mm			
D_{AP}	26.92 ± 2.02	27.88 ± 2.03	0.150
D_{AL}	47.71 ± 5.51	49.06 ± 5.73	0.458
D_{AM}	50.88 ± 5.38	52.13 ± 5.16	0.469
D_{PL}	46.63 ± 4.42	47.81 ± 6.12	0.480
D_{PM}	46.42 ± 4.79	46.38 ± 4.87	0.979
D_{ML}	20.29 ± 2.65	25.38 ± 5.92	0.004[a]

Abbreviations: D_{AL}, the distance between the root of lateral papillary muscle and the anterior annulus; D_{AM}, the distance between the root of medial papillary muscle and the anterior annulus; D_{AP}, distance between the anterior and posterior annulus; D_{ML}, the interpapillary muscle roots distance; D_{PL}, the distance between the root of lateral papillary muscle and the posterior annulus; D_{PM}, the distance between the root of medial papillary muscle and the posterior annulus; ERO, effective regurgitant orifice; LVEDV, left ventricular end-diastolic volume; LVEF, left ventricular ejection fraction; LVESV, left ventricular end-systolic volume.
Data are presented as mean $\pm$ standard deviation.
[a]$P < 0.05$ indicates a significant difference between ERO levels.

Discussion

This study demonstrated that significant ischemic MR occurred in more than one-third of patients with a previous myocardial infarction, especially the patients with inferior wall MI. The increase of ERO was associated with an increase of systolic mitral valvular tenting, LV end-diastolic volume, sphericity of the LV, and interpapillary muscle distance. The major determinant of significant IMR is the systolic mitral valvular tenting along with interpapillary muscle distance. The findings of this study provided possible targets to ameliorate IMR.

Mitral Tetrahedron

The presence of IMR after MI or in ischemic cardiomyopathy has an adverse prognosis.[2–4,24] The primary goal of current studies is to elucidate the mechanism of IMR and develop an appropriate treatment modality. Several mechanisms have been proposed such as mitral valve tethering due to global LV dilatation or local LV remodeling, mitral annular dilatation or loss of annular contraction, and LV systolic dysfunction.[6,11–15,25] However, the variables in these studies, such as tethering distance, papillary muscle displacement, and mitral annular diameter, have mostly been assessed by 2D echocardiography. These 2D imaging

Published online in Wiley Online Library (wileyonlinelibrary.com)
DOI:10.1002/clc.22111

Table 4. Correlation of ERO With Echocardiographic Variables

Echocardiographic Variables	ERO, mm² (*r*)	*P* Value
Tenting area, cm²	0.574	< 0.001[a]
Mitral annular area, cm²	0.207	0.201
LVEDV, mL	0.352	0.026[a]
LVESV, mL	0.294	0.066
Spherical index at systole	0.458	0.003[a]
LVEF, %	−0.279	0.081
Edge length of mitral tetrahedron, mm		
D_{AP}	0.145	0.370
D_{AL}	0.206	0.202
D_{AM}	0.209	0.196
D_{PL}	0.186	0.251
D_{PM}	0.075	0.645
D_{ML}	0.449	0.004[a]

Abbreviations: D_{AL}, the distance between the root of lateral papillary muscle and the anterior annulus; D_{AM}, the distance between the root of medial papillary muscle and the anterior annulus; D_{AP}, distance between the anterior and posterior annulus; D_{ML}, the interpapillary muscle roots distance; D_{PL}, the distance between the root of lateral papillary muscle and the posterior annulus; D_{PM}, the distance between the root of medial papillary muscle and the posterior annulus; ERO, effective regurgitant orifice; LVEDV, left ventricular end-diastolic volume; LVEF, left ventricular ejection fraction; LVESV, left ventricular end-systolic volume.
Results are expressed as coefficients of Pearson correlation analysis.
[a]Indicates a significant correlation.

planes may miss the true distance and cannot realize the spatial relationship. Yu et al. utilized MRI, which can translate the data into 3D information, and proposed the mitral tetrahedron as a method to assess the relation of LV remodeling with mitral apparatus and IMR.[17] A mitral tetrahedron is defined by its 4 vertices at the medial, lateral papillary muscle roots, and the anterior and posterior mitral annulus (Figure 1). One pertinent difference in the methodology of this study was that the roots of papillary muscle rather than the tips were used as measurement points. This was because the tips of papillary muscle are branched and the connection point of the chordae tendinea and the tips of papillary muscle are not clear, which may interfere with the measurement. Nonetheless, MRI cannot quantify the degree of IMR and cannot precisely delineate mitral valvular deformation such as tenting area and coaptation height. Advancements in 3D echocardiography allow assessment of the spatial relationship of the LV and mitral apparatus. In the present study, we demonstrated the measurement of the mitral tetrahedron by 3D echocardiography. Thus, we compared mitral valvular deformity, the severity of ERO, and the mitral tetrahedron by 2D and 3D echocardiography simultaneously. This provided a novel and convenient method for studying the mechanism of IMR. Compared with the study by Yu et al.,[18] the present study evaluated patients in the relatively early stage of IMR and facilitated in deducing the possible initial trigger because of "MR begets MR." We showed that the interpapillary distance may be the most significant factor in the early stages of LV remodeling.

Determinants of IMR

The generation of IMR is involved with several mechanisms; although, incomplete closure of the normal mitral leaflet is currently thought to be the main cause.[10,11,26] Additional mechanisms include LV dilatation, LV systolic dysfunction, and mitral annular dilatation.[13,15,25] Several recent studies postulated that LV remodeling caused displacement of papillary muscles, and resultant tethering of mitral leaflets restricts the closure of mitral leaflets and results in mitral valvular tenting. The systolic mitral valvular tenting correlated well with ERO. LV dilatation and annular dilatation demonstrated a minor role in the determination of IMR.[13,15,26]

In the present study, we also demonstrated that the strongest correlation with ERO is systolic mitral valvular tenting. The degree of LV enlargement was a minor factor in producing IMR, and LV dysfunction was not associated with IMR. One inconsistency with previous studies is that the mitral annular area did not correlate with ERO, although it had a good association with the mitral tenting area (Supplementary Table 1). Because the ratio of leaflets to annular area is >2,[27] if the annulus is not large enough, incomplete coaptation of mitral leaflets will not occur.[28] This may explain why annular size played a minor role in causing IMR in some studies.[25,28,29] The relatively small annular size in this study, presumably due to less severe disease, may be why there was no correlation between the mitral annular area and ERO.

Most studies confirmed that mitral valve tenting can predict IMR,[13,15,26] and a recent study reveled that only increased tenting area was predictive of progression of MI over time,[30] but these studies have rarely mentioned or investigated the role of interpapillary muscle distance in IMR. Our study provides new information about factors that may contribute to IMR. We demonstrated that besides mitral valvular tenting, interpapillary muscle distance is strongly correlated with ERO, and as such is an independent predictor of significant IMR. Papillary muscle separation may cause tethering of both leaflets toward the direction parallel to the coaptation line and distort the coaptation geometry,[17,29,31] lessening the force for mitral valve coaptation and resulting in incomplete closure of normal mitral leaflets. Because an increase in mitral valvular tenting reflects apical tethering of the mitral valve, and an increase in the interpapillary muscle distance causes medial-lateral tethering of the mitral valve (leading to poor coaptation near the central mitral valve), it is apparent that abnormalities in either of these anatomical factors can contribute to the likelihood of IMR. In this study, LV remodeling, either after anterior MI or inferior MI, involving papillary muscle separation led to significant MR. The stepwise regression analysis demonstrated that the interpapillary muscle distance also determines the severity of IMR beyond the tenting area. For those cases having the same tenting area, the increased interpapillary muscle distance will lessen the force of mitral valve coaptation.

Unlike the results of previous studies,[16,17] this study showed that only D_{ML} was associated with MR severity.

Published online in Wiley Online Library (wileyonlinelibrary.com)
DOI:10.1002/clc.22111

Table 5. Risk Factors Associated With Significant Ischemic Mitral Regurgitation

Variables	Univariate, OR (95% CI)	*P* Value	Multivariate, OR (95% CI)	*P* Value
Tenting area, cm^2	181.95 ($7.275\text{-}4.55 \times 10^3$)	0.002[a]	280.49 ($4.59\text{-}1.72 \times 10^4$)	0.007[a]
Mitral annular area, cm^2	1.007 (1.000-1.015)	0.043[a]	—	
LVEDV, mL	1.030 (0.999-1.062)	0.061	—	
LVESV, mL	1.040 (0.998-1.084)	0.063	—	
Spherical index at systole	6.8×10^4 ($12.749\text{-}3.67 \times 10^8$)	0.011[a]	—	
LVEF, %	0.927 (0.863-0.995)	0.036[a]	—	
Edge length of mitral tetrahedron, mm			—	
D_{AP}	1.271 (0.914-1.767)	0.154	—	
D_{AL}	1.046 (0.932-1.174)	0.448	—	
D_{AM}	1.048 (0.926-1.185)	0.459	—	
D_{PL}	1.048 (0.924-1.188)	0.470	—	
D_{PM}	0.998 (0.872-1.142)	0.978	—	
D_{ML}	1.371 (1.083-1.737)	0.009[a]	1.50 (1.03-2.19)	0.036[a]

Abbreviations: D_{AL}, the distance between the root of lateral papillary muscle and the anterior annulus; D_{AM}, the distance between the root of medial papillary muscle and the anterior annulus; D_{AP}, distance between the anterior and posterior annulus; D_{ML}, the interpapillary muscle roots distance; D_{PL}, the distance between the root of lateral papillary muscle and the posterior annulus; D_{PM}, the distance between the root of medial papillary muscle and the posterior annulus; ERO, effective regurgitant orifice; LVEDV, Left ventricular end-diastolic volume; LVEF, left ventricular ejection fraction; LVESV, left ventricular end-systolic volume.
Results are expressed as odds ratio (OR) with respective 95% confidence interval (95% CI) and *P* value.
[a] $P < 0.05$.

Failure to demonstrate an association of factors other than D_{ML} with MR may be due to the fact that the subject population consisted of earlier stage MR, and that LV remodeling was also in the early stage. Relatively speaking, the absence of a statistically significant association between the other 5 edge lengths and MR severity may be interpreted to indicate that D_{ML} is the most important and the earliest factor influencing the development of MR.

The pattern of mitral tenting might also be a determinant in IMR severity. A recent study comparing the MR caused by ischemic heart disease and by dilated cardiomyopathy found that with the same increment of mitral valvular tenting area, MR is more severe if the pattern of mitral valvular deformity is asymmetrical. The asymmetrical tethering causes poor coaptation and greater incomplete closure of mitral leaflets and subsequently more severe MR.[32] This explains the higher prevalence of IMR in patients with inferior MI than in those with anterior MI in this and previous studies; although, the mitral valvular tenting area is similar between patients with anterior MI and inferior MI in our study (Supplementary Table 2).

Clinical Implications

Ring annuloplasty for annular size reduction is the current surgical procedure for IMR. However, persistent MR and high recurrent rates at long-term follow-up visits have been reported.[33–35] Our data demonstrated that annular enlargement per se is not the major cause of IMR. Future surgical intervention may focus on the correction of papillary muscle separation and the causes of mitral valvular tenting, such as leaflet tethering, to improve the coaptation of mitral leaflets. Routine 3D echocardiography for measurement of mitral tetrahedron in evaluation of IMR may help to determine the cause and subsequent selection of the treatment method.

Study Limitations

In the present study, we used the concept of the mitral tetrahedron to assess the geometric change of the LV. The true tethering distance could not be recognized with this method. Moreover, the resolution of the 3D echocardiographic images was relatively low. The relatively long period of time that elapsed between when patients were recruited for this study (ie, 2005–2006) and when the results were first submitted for publication, meant that relatively old imaging software (eg, QLAB 4.1) was used when this study was conducted. In the interim, the imaging software has been updated (eg, QLAB 9.0). Further advances in 3D echocardiography imaging software and offline analysis may improve the measurement of the mitral tetrahedron. Additionally, we did not address the pattern of the mitral valvular deformity in the present study. Further studies are warranted to understand the relationship of the pattern of mitral valvular deformity and the mitral tetrahedron along with the location of the MR, which may help delineate the mechanism of FMR. The study population was small, and consisted of both patients with normal ejection fraction (EF) and patients with reduced EF. Further investigations with a larger study population, in which a more detailed subgroup analysis can be conducted, are required to confirm the results of this

Published online in Wiley Online Library (wileyonlinelibrary.com)
DOI:10.1002/clc.22111

study. Information regarding the measurement of papillary muscle root distance on 2D images was not obtained in this study. However, future studies can potentially use the findings of this study as a basis for comparing 2D and 3D measurements of interpapillary muscle distance and their association with various factors.

Conclusion

In this study, we demonstrated that real-time 3D echocardiography was capable of measuring the mitral tetrahedron. Interpapillary muscle distance was the independent determinant of significant IMR in addition to mitral valvular tenting. The methods and findings of this study may be applicable to clinical use and help develop new surgical approaches for treatment of IMR.

References

1. Borger MA, Alam A, Murphy PM, et al. Chronic ischemic mitral regurgitation: repair, replace or rethink? *Ann Thorac Surg*. 2006;81:1153–1161.
2. Bursi F, Enriquez-Sarano M, Nkomo VT, et al. Heart failure and death after myocardial infarction in the community: the emerging role of mitral regurgitation. *Circulation*. 2005;111:295–301.
3. Grigioni F, Detaint D, Avierinos JF, et al. Contribution of ischemic mitral regurgitation to congestive heart failure after myocardial infarction. *J Am Coll Cardiol*. 2005;45:260–267.
4. Grigioni F, Enriquez-Sarano M, Zehr KJ, et al. Ischemic mitral regurgitation: long-term outcome and prognostic implications with quantitative Doppler assessment. *Circulation*. 2001;103:175917–175964.
5. Burch GE, De Pasquale NP, Phillips JH. Clinical manifestations of papillary muscle dysfunction. *Arch Intern Med*. 1963;112:112–117.
6. Izumi S, Miyatake K, Beppu S, et al. Mechanism of mitral regurgitation in patients with myocardial infarction: a study using real-time two-dimensional Doppler flow imaging and echocardiography. *Circulation*. 1987;76:777–785.
7. Messas E, Guerrero JL, Handschumacher MD, et al. Paradoxic decrease in ischemic mitral regurgitation with papillary muscle dysfunction: insights from three-dimensional and contrast echocardiography with strain rate measurement. *Circulation*. 2001;104:1952–1957.
8. Mittal AK, Langston M Jr, Cohn KE, et al. Combined papillary muscle and left ventricular wall dysfunction as a cause of mitral regurgitation. An experimental study. *Circulation*. 1971;44:174–180.
9. Uemura T, Otsuji Y, Nakashiki K, et al. Papillary muscle dysfunction attenuates ischemic mitral regurgitation in patients with localized basal inferior left ventricular remodeling: insights from tissue Doppler strain imaging. *J Am Coll Cardiol*. 2005;46:113–119.
10. Godley RW, Wann LS, Rogers EW, et al. Incomplete mitral leaflet closure in patients with papillary muscle dysfunction. *Circulation*. 1981;63:565–571.
11. He S, Fontaine AA, Schwammenthal E, et al. Integrated mechanism for functional mitral regurgitation: leaflet restriction versus coapting force: in vitro studies. *Circulation*. 1997;96:1826–1834.
12. Kaul S, Spotnitz WD, Glasheen WP, et al. Mechanism of ischemic mitral regurgitation. *An experimental evaluation. Circulation*. 1991;84:2167–2180.
13. Kumanohoso T, Otsuji Y, Yoshifuku S, et al. Mechanism of higher incidence of ischemic mitral regurgitation in patients with inferior myocardial infarction: quantitative analysis of left ventricular and mitral valve geometry in 103 patients with prior myocardial infarction. *J Thorac Cardiovasc Surg*. 2003;125:135–143.
14. Otsuji Y, Handschumacher MD, Liel-Cohen N, et al. Mechanism of ischemic mitral regurgitation with segmental left ventricular dysfunction: three-dimensional echocardiographic studies in models of acute and chronic progressive regurgitation. *J Am Coll Cardiol*. 2001;37:641–648.
15. Yiu SF, Enriquez-Sarano M, Tribouilloy C, et al. Determinants of the degree of functional mitral regurgitation in patients with systolic left ventricular dysfunction: a quantitative clinical study. *Circulation*. 2000;102:1400–1406.
16. Zakkar M, Patni R, Punjabi PP. Mitral valve regurgitation and 3D echocardiography. *Future Cardiol*. 2010;6:231–242.
17. Yu HY, Su MY, Liao TY, et al. Functional mitral regurgitation in chronic ischemic coronary artery disease: analysis of geometric alterations of mitral apparatus with magnetic resonance imaging. *J Thorac Cardiovasc Surg*. 2004;12:543–551.
18. Yu HY, Su MY, Chen YS, et al. Mitral tetrahedron as a geometrical surrogate for chronic ischemic mitral regurgitation. *Am J Physiol Heart Circ Physiol*. 2005;289:H1218–H1225.
19. Schiller NB, Shah PM, Crawford M, et al. Recommendations for quantitation of the left ventricle by two-dimensional echocardiography. American Society of Echocardiography Committee on Standards, Subcommittee on Quantitation of Two-Dimensional Echocardiograms. *J Am Soc Echocardiogr*. 1989;2:358–367.
20. D'Cruz IA, Shroff SG, Janicki JS, et al. Differences in the shape of the normal, cardiomyopathic, and volume overloaded human left ventricle. *J Am Soc Echocardiogr*. 1989;2:408–414.
21. Blumlein S, Bouchard A, Schiller NB, et al. Quantitation of mitral regurgitation by Doppler echocardiography. *Circulation*. 1986;74:306–314.
22. Enriquez-Sarano M, Bailey KR, Seward JB, et al. Quantitative Doppler assessment of valvular regurgitation. *Circulation*. 1993;87:841–848.
23. Enriquez Sarano M, Seward JB, Bailey KR, Tajik AJ. Effective regurgitant orifice area: a noninvasive Doppler development of an old hemodynamic concept. *J Am Coll Cardiol*. 1994;23:443–451.
24. Fernandez-Golfin C, De Agustin A, Manzano MC, et al. Cardiac magnetic resonance determinants of functional mitral regurgitation in ischemic and non-ischemic lest ventricular dysfunction. *Int J Cardiovasc Imaging*. 2011;27:539–546.
25. Daimon M, Saracino G, Fukuda S, et al. Dynamic change of mitral annular geometry and motion assessed by a computerized 3D Echo Method. *Echocardiography*. 2010;27:1069–1077.
26. Watanabe N, Ogasawara Y, Yamaura Y, et al. Quantitation of mitral regurgitation by transthoracic real-time three-dimensional echocardiography. *J Am Coll Cardiol*. 2005;45:763–769.
27. Perloff JK, Roberts WC. The mitral apparatus: functional anatomy of mitral regurgitation. *Circulation*. 1972;46:227–239.
28. Sadeghpour A, Abtahi F, Kiavar M, et al. Echocardiographic evaluation of mitral geometry in functional mitral regurgitation. *J Cardiothorac Surg*. 2008;3:54.
29. Kwan J, Gillinov MA, Thomas JD, et al. Geometric predictor of significant mitral regurgitation in patients with severe ischemic cardiomyopathy, undergoing Dor procedure: a real-time 3D echocardiographic study. *Eur J Echocardiography*. 2007;8:195–203.
30. Meris A, Amigoni M, Verma A, et al. Mechanisms and predictors of mitral regurgitation after high-risk myocardial infarction. *J Am Soc Echocardiogr*. 2012;25:535–542.
31. Jorapur V, Voudouris A, Lucariello RJ. Quantification of annular dilatation and papillary muscle separation in functional mitral regurgitation: role of anterior mitral leaflet length as reference. *Echocardiography*. 2005;22:465–472.
32. Kwan J, Shiota T, Agler DA, et al. Real-time three-dimensional echocardiography study: geometric differences of the mitral apparatus between ischemic and dilated cardiomyopathy with significant mitral regurgitation: real-time three-dimensional echocardiography study. *Circulation*. 2003;107:1135–1140.
33. Hung J, Papakostas L, Tahta SA, et al. Mechanism of recurrent ischemic mitral regurgitation after annuloplasty: continued LV remodeling as a moving target. *Circulation* 2004;110(11 suppl 1):II85–II90.
34. McGee EC Jr, Gillinov AM, Blackstone EH, et al. Recurrent mitral regurgitation after annuloplasty for functional ischemic mitral regurgitation. *J Thorac Cardiovasc Surg*. 2004;2128: 916–924.
35. Tahta SA, OuryJH, Maxwell JM, et al. Outcome after mitral valve repair for functional ischemic mitral regurgitation. *J Heart Valve Dis*. 2002;11:11–19.

Published online in Wiley Online Library (wileyonlinelibrary.com)
DOI:10.1002/clc.22111